

# Self-oscillations in a superconducting stripline resonator integrated with a dc superconducting quantum interference device

Eran Segev,<sup>a)</sup> Oren Suchoi, Oleg Shtempluck, and Eyal Buks  
*Department of Electrical Engineering, Technion, Haifa 32000, Israel*

(Received 23 July 2009; accepted 20 September 2009; published online 14 October 2009)

We study self-sustained oscillations in a Nb superconducting stripline resonator integrated with a dc superconducting quantum interference device (SQUID). We find that both the power threshold where these oscillations start and the oscillation frequency are periodic in the applied magnetic flux threading the SQUID loop. A theoretical model which attributes the self-sustained oscillations to a thermal instability in the dc-SQUID yields a good agreement with the experimental results. This flux dependant nonlinearity may be used for quantum state reading of a qubit-superconducting resonator integrated device. © 2009 American Institute of Physics. [doi:10.1063/1.3250167]

We study thermal instability in superconducting stripline resonators (SSRs) working at gigahertz frequencies. We have recently demonstrated how thermal instability can create extremely strong nonlinearity in such resonators.<sup>1,2</sup> This nonlinearity is manifested by self-sustained oscillations (SOs) at megahertz frequencies, strong intermodulation gain, stochastic resonance, sensitive radiation detection, and more.<sup>3</sup> In the present work we have integrated a SSR with a dc superconducting quantum interference device (SQUID). Similar configurations have been recently studied by other groups and it was shown that such devices can be used as readout and coupling elements for qubits.<sup>4-6</sup> In addition, it was shown that further improvement in the sensitivity of the readout process of the qubit is possible by biasing the resonator to a state of nonlinear responsivity.<sup>5-9</sup>

Our experiments are performed using the setup depicted in Fig. 1(a). We study the response of the integrated SSR to a monochromatic injected pump tone that drives one of the resonance modes, and measure the reflected power spectrum by a spectrum analyzer. We find that there is a certain range in the plane of the pump-frequency pump-power parameters, in which intrinsic SOs occur in the resonator. These oscillations are manifested by the appearance of sidebands in the reflected power spectrum. In addition, we apply bias magnetic flux through the dc-SQUID and find that both the threshold where these oscillations start and their frequency are periodic in the applied magnetic flux, having a periodicity of one flux quantum. We extend our theoretical model,<sup>1</sup> which has originally considered SOs and thermal instability in a SSR integrated with a single microbridge to include this flux dependency and find a good agreement with the experimental results.

A simplified circuit layout of our device is illustrated in Fig. 1(b). We fabricate our devices on a silicon wafer, covered by a thin layer of silicon nitride. Each device is made of a thin layer (<100 nm) of niobium and composed of a stripline resonator having a dc-SQUID [Fig. 1(c)] monolithically embedded into its structure. The resonator length is  $l=18$  mm and its first resonance mode is found at  $f_1 = \omega_1/2\pi = 3.006$  GHz. The dc-SQUID has two nanobridges [Fig. 1(d)], one in each of its two arms. Their size is typically

100 nm<sup>2</sup> and therefore each nanobridge functions as a weak link that approximately can be regarded as a regular Josephson junction.<sup>10,11</sup> A feed line, weakly coupled to the resonator, is employed for delivering the input and output signals. An on-chip filtered dc bias line passes near the dc-SQUID and is used to apply magnetic flux through the SQUID. Some measurements are carried out while the device is fully immersed in liquid helium, while others in a dilution refrigerator where the device is in vacuum. Further design considerations and fabrication details can be found elsewhere.<sup>12</sup>

Figure 2 exhibits SOs in the power reflected off the resonator.<sup>1,13</sup> In this measurement we inject into the resonator an input pump tone having a monochromatic frequency  $\omega_p = \omega_1$  and measure the reflected power spectrum around  $\omega_1$ , while varying the input pump power  $P_p$ . At relatively low ( $P_p \lesssim -66$  dBm) and high ( $P_p \gtrsim -48$  dBm) pump powers the response of the resonator is linear, namely, the reflected power spectrum contains a single spectral component at the frequency of the stimulating pump tone. In between these two power thresholds the resonator self oscillates and regular modulation of the pump tone occurs. As a result, the reflected spectrum contains several orders of modulation products realized by rather strong and sharp sidebands (see inset of Fig. 2) that extend to both sides of the pump tone frequency. The SO frequency, defined as the frequency differ-

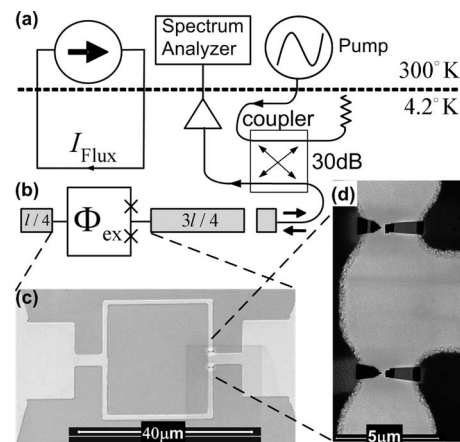


FIG. 1. (a) Measurement setup. (b) Schematic layout of our device (not scaled). (c) SEM image of the dc-SQUID. (d) SEM image of the two nanobridge-based Josephson junctions.

<sup>a)</sup>Electronic mail: segev@tx.technion.ac.il.

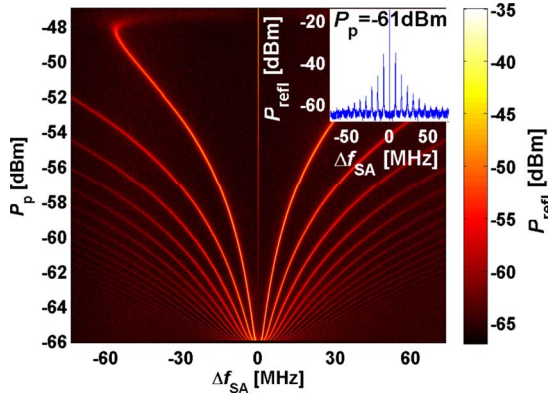


FIG. 2. (Color online) Typical experimental results of the SO phenomenon. The color map shows the reflected power  $P_{\text{refl}}$  as a function of the input pump power  $P_p$  and the measured frequency  $f_{\text{SA}}$ , centered on the pump frequency, which coincides with the first resonance frequency  $f_1$  ( $\Delta f_{\text{SA}} = f_{\text{SA}} - f_1$ ). Note that the data is truncated at  $P_{\text{refl}} = -35$  dBm for clarity. The inset shows a section of that measurement obtained with  $P_p = -61$  dBm.

ence between the pump frequency and the primary sideband, ranges from few to tens of megahertz and increases with the pump power.

The dependence of the SOs on the applied magnetic flux is shown in Fig. 3. In this measurement we inject a pump tone having a stationary frequency ( $\omega_p \approx \omega_1$ ) and power ( $P_p = -51.5$  dBm), and measure the reflected power spectrum around  $\omega_1$ , while varying the dc bias current. As shown, the SO frequency is periodically changed by the applied magnetic flux. The periodicity is one flux quantum and the relative change is typically about 20%. Figures 4(a) and 4(c) show two measurements of flux dependent SOs obtained with pump power above and equal to the threshold power ( $P_{p,(a)} = -51.5$  dBm,  $P_{p,(c)} = -51.6$  dBm), respectively. The later measurement demonstrates how magnetic flux can switch the resonator from a steady state response to a limit-cycle state where it experiences the SOs.

To account for our results we model our device as a transmission line resonator interrupted by a dc-SQUID. The impedance of the dc-SQUID is composed of a constant inductor in series with a flux-dependent inductor shunted by a parallel resistor.<sup>12</sup> The flux dependence of the dc-SQUID impedance gives rise to periodic dependence of the SSR damping rates on the applied magnetic field (the change in the SSR resonance frequency is relatively small).

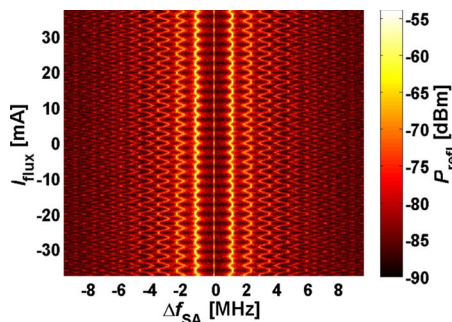


FIG. 3. (Color online) Typical experimental results of flux dependent SOs. The color map shows the reflected power  $P_{\text{refl}}$  as a function of the bias dc current  $I_{\text{flux}}$  and the measured frequency  $f_{\text{SA}}$  centered on the pump frequency  $f_p = f_1$  ( $\Delta f_{\text{SA}} = f_{\text{SA}} - f_1$ ).

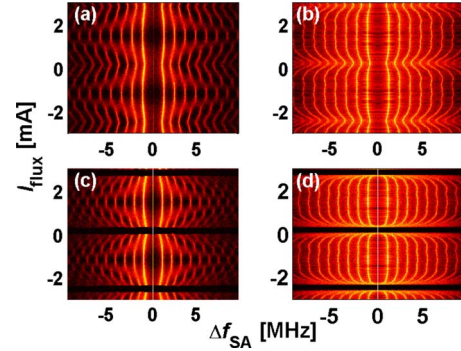


FIG. 4. (Color online) Typical experimental and numerical results of flux dependent SOs. Each panel shows a color map of the reflected power  $P_{\text{refl}}$  as a function of the bias dc current  $I_{\text{flux}}$  and the measured frequency  $f_{\text{SA}}$  centered on the pump frequency  $f_p = f_1$  ( $\Delta f_{\text{SA}} = f_{\text{SA}} - f_1$ ). Panels [(a) and (c)] show experimental results obtained at pump power above and equal to the low threshold power, respectively. Panels [(b) and (d)] show the corresponding theoretical results obtained by numerically integrating the equations of motion.

The dynamics of our system can be captured thus by two coupled equations of motion.<sup>1</sup> The first equation describes the dynamics of a resonator driven by feed line carrying an incident coherent tone  $b^{\text{in}} = b_0^{\text{in}} e^{-i\omega_p t}$ , where  $b_0^{\text{in}}$  is constant complex amplitude and  $\omega_p = 2\pi f_p$  is the driving angular frequency. The mode amplitude inside the resonator can be written as  $B e^{-i\omega_p t}$ , where  $B(t)$  is complex amplitude, which is assumed to vary slowly on a time scale of  $1/\omega_p$ . In this approximation, assuming a noiseless system, the equation of motion of  $B$  reads<sup>14</sup>

$$\frac{dB}{dt} = [i(\omega_p - \omega_0) - \gamma]B - i\sqrt{2}\gamma_1 b^{\text{in}}, \quad (1)$$

where  $\omega_0$  is the angular resonance frequency and  $\gamma(T) = \gamma_1 + \gamma_2(T, \Phi_{\text{ex}})$ , where  $\gamma_1$  is the coupling coefficient between the resonator and the feed line and  $\gamma_2(T, \Phi_{\text{ex}})$  is the temperature and flux dependent damping rate of the mode.

The heat-balance equation for the temperature  $T$  of the nanobridges composing the dc-SQUID is given by<sup>13</sup>

$$C \frac{dT}{dt} = 2\hbar\omega_0\gamma_2|B|^2 - H(T - T_0), \quad (2)$$

where  $C$  is the thermal heat capacity,  $H$  is the heat transfer coefficient, and  $T_0$  is the temperature of the coolant.

Coupling between Eqs. (1) and (2) originates by the dependence of the damping rate  $\gamma_2(T, \Phi_{\text{ex}})$  of the driven mode on the impedance of the dc-SQUID,<sup>15</sup> which in turn depends on the temperature of its nanobridges and on the applied magnetic flux. We assume a simple case, where the dependence on the temperature  $T$  is described by a step function that occurs at the critical temperature  $T_c$  of the superconductor. We further assume that only when the nanobridges are in a superconducting phase the damping rate depends on the external flux. Namely,  $\gamma_2$  takes a flux dependent value  $\gamma_{2s}(\Phi_{\text{ex}})$  when the nanobridges are in a superconducting phase ( $T < T_c$ ) and a flux-independent value  $\gamma_{2n}$  when they are in a normal-conducting phase ( $T > T_c$ ).

The results of a numerical integration of the equations of motion are shown in Figs. 4(b) and 4(d). Our model qualitatively reproduces the same flux dependency of the SO frequency on the magnetic flux. The parameters used for the

numerical simulation were obtained as follows. The thermal heat capacity  $C=4.5 \text{ nJ cm}^{-2} \text{ K}^{-1}$  and the heat transfer coefficient  $H=24.5 \text{ mW cm}^{-2} \text{ K}^{-1}$  were calculated analytically according to Refs. 16 and 17. The values of the resonance frequency and the various damping rates,  $\gamma_{1s}=2.4 \text{ MHz}$ ,  $\gamma_{2s} \in [2.93, 3.32] \text{ MHz}$ ,  $\gamma_{2n}=13 \text{ MHz}$ , and  $\omega_0=2\pi \cdot 3.006 \text{ GHz}$  were extracted from S11 reflection coefficient measurements according to Ref. 18.

In conclusion, we report on periodic flux-dependency of SOs in a SSR integrated with a dc-SQUID. The flux significantly modulates the oscillation frequency and can be used to turn them on and off if the device is driven near the power threshold. A theoretical model which attributes this behavior to thermal instability in the dc-SQUID exhibits a good quantitative agreement with the experimental results.

We thank Steve Shaw for valuable discussions and helpful comments. E.S. is supported by the Adams Fellowship Program of the Israel Academy of Sciences and Humanities. This work is supported by the German Israel Foundation under Grant No. 1-2038.1114.07, the Israel Science Foundation under Grant No. 1380021, the Deborah Foundation, the Poznanski Foundation, Russell Berrie nanotechnology institute, and MAFAT.

<sup>1</sup>E. Segev, B. Abdo, O. Stempluk, and E. Buks, *J. Phys.: Condens. Matter* **19**, 096206 (2007).

<sup>2</sup>E. Segev, B. Abdo, O. Stempluk, and E. Buks, *Phys. Rev. B* **77**, 012501 (2008).

<sup>3</sup>G. Bachar, E. Segev, B. Abdo, O. Stempluk, S. W. Shaw, and E. Buks, arXiv:0810.0964v2.

<sup>4</sup>A. Wallraff, D. I. Schuster, A. Blais, L. Frunzio, R.-S. Huang, J. Majer, S. Kumar, S. M. Girvin, and R. J. Schoelkopf, *Nature (London)* **431**, 162 (2004).

<sup>5</sup>A. Lupascu, E. F. C. Driessen, L. Roschier, C. J. P. M. Harmans, and J. E. Mooij, *Phys. Rev. Lett.* **96**, 127003 (2006).

<sup>6</sup>J. C. Lee, W. D. Oliver, K. K. Berggren, and T. P. Orlando, *Phys. Rev. B* **75**, 144505 (2007).

<sup>7</sup>I. Siddiqi, R. Vijay, M. Metcalfe, E. Boaknin, L. Frunzio, R. J. Schoelkopf, and M. H. Devoret, *Phys. Rev. B* **73**, 054510 (2006).

<sup>8</sup>E. Boaknin, V. Manucharyan, S. Fissette, M. Metcalfe, L. Frunzio, A. Wallraff, R. J. Schoelkopf, and M. Devoret, arXiv:cond-mat/0702445v1.

<sup>9</sup>M. Metcalfe, E. Boaknin, V. Manucharyan, R. Vijay, I. Siddiqi, C. Rigetti, L. Frunzio, R. J. Schoelkopf, and M. H. Devoret, *Phys. Rev. B* **76**, 174516 (2007).

<sup>10</sup>A. G. P. Troeman, S. H. W. V. der Ploeg, E. Il'ichev, H. G. Meyer, A. A. Golubov, M. Y. Kupriyanov, and H. Hilgenkamp, *Phys. Rev. B* **77**, 024509 (2008).

<sup>11</sup>A. G. P. Troeman, H. Derking, B. Borgerm, J. Pleikies, D. Veldhuis, and H. Hilgenkamp, *Nano Lett.* **7**, 2152 (2007).

<sup>12</sup>O. Suchoi, B. Abdo, E. Segev, O. Shtempluck, M. P. Blencowe, and E. Buks, arXiv:0901.3110v1.

<sup>13</sup>E. Segev, B. Abdo, O. Shtempluck, and E. Buks, *Europhys. Lett.* **78**, 57002 (2007).

<sup>14</sup>B. Yurke and E. Buks, *J. Lightwave Technol.* **24**, 5054 (2006).

<sup>15</sup>D. Saeedkia, A. H. Majedi, S. Safavi-Naeini, and R. R. Mansour, *IEEE Microw. Wirel. Compon. Lett.* **15**, 510 (2005).

<sup>16</sup>M. W. Johnson, A. M. Herr, and A. M. Kadin, *J. Appl. Phys.* **79**, 7069 (1996).

<sup>17</sup>K. Weiser, U. Strom, S. A. Wolf, and D. U. Gubser, *J. Appl. Phys.* **52**, 4888 (1981).

<sup>18</sup>E. Arbel-Segev, B. Abdo, O. Shtempluck, and E. Buks, *IEEE Trans. Appl. Supercond.* **16**, 1943 (2006).